

Chapter 17

Near Field Flow Dynamics of Concentrate Discharges and Diffuser Design

Philip J.W. Roberts

Abstract The major physical aspects of near field mixing of dense jets resulting from diffuser discharges of concentrate are presented. It is proposed that any environmental impacts of such discharges will be local rather than regional, so initial mixing processes are an essential component of an effective disposal scheme. Typical international environmental criteria for concentrate are summarized; these can be readily met by well-designed diffusers. The major features of dense jets are presented, beginning with the simplest case of an inclined jet into deep stationary water, followed by the effects of shallow water. We then discuss merging jets from multiport and rosette diffusers and it is shown that their dynamic interaction can be critical and lead to significant changes in flow patterns and reduction in dilution. Design criteria are suggested to avoid impaired dilution. The effects of currents on single and multiport diffusers are then discussed. It is shown that small modifications in diffuser design can lead to significant changes in flow field and dilution. Some issues and difficulties with mathematical modeling of near field flows are discussed and how entrainment models may not adequately represent critical phenomena including dynamic jet and boundary interaction, re-entrainment, density current dynamics, and turbulence collapse. Finally, some open research issues are discussed.

17.1 Introduction

Concentrate resulting from seawater desalination can be safely discharged back to the ocean with minimal environmental impact if adequately diluted near to the source. This dilution can be accomplished by many means, of which a diffuser

P.J.W. Roberts (✉)
Georgia Institute of Technology, Atlanta, USA
e-mail: proberts@ce.gatech.edu

is one. The objective of a diffuser is rapid dilution and mixing of the concentrate to reduce salinity to near background levels. The environmental impacts of well-designed operating diffusers have been studied in extensive field observations in Australia which show that any observable effects are confined to a small region, of order tens of meters from the diffuser (Roberts et al. 2010).

This might be expected when considering the primary processes involved in seawater desalination and their hydrometeorological fluxes. Desalination takes in seawater, concentrates it, and returns it to the ocean with no net addition of salt. There is some abstraction of freshwater, however, which could potentially lead to increases in background salinity.

These impacts will generally be very small and localized as can be illustrated by considering desalination effects on the Gulf of Arabia. The Gulf evaporates by about 1.5 m/year (Smith et al. 2007) (the Red Sea evaporates by about 2 m/year, Sofianos et al. 2002). The Gulf's surface area is about 250,000 km², therefore this evaporation corresponds to a freshwater abstraction of about 12,000 m³/s. Total desalination production in the Gulf is currently of order 150 m³/s (Lattemann and Höpner 2008). As this is very small (order 1 %) compared to evaporation, its effect would be swamped by natural variability and extremely difficult, if not impossible, to measure. Even anticipated future growth would not cause this effect to become significant. It is therefore clear that regional impacts should be minor. Similar conclusions would be expected for other coastal regions, where oceanographic fluxes far exceed those due to desalination plants.

Almost by definition then, any effects should be local, or near field, so providing rapid initial dilution should mitigate any environmental impacts of salinity. Of course, there are other potential effects such as from disposal of filter backwash or chemicals added during the desalination process as discussed by, for example, Lattemann and Höpner (2008). It has also been suggested that mortality of organisms due to turbulence and shear in the diffuser jets may also be a factor. We don't discuss these issues here as this chapter is concerned with the fluid mechanical aspects of near field mixing of typical brine diffusers and their design to meet environmental criteria.

Of course, there are other means of concentrate disposal, such as co-disposal with power plant cooling water whose volumes, particularly those associated with once-through cooling, are generally much greater than those due to desalination plants. Once-through cooling is being phased out in California, however, mainly because of its effect on entrained organisms and this may not be an option in the future.

The outline of this chapter is as follows. We first discuss typical regulatory criteria that apply to brine diffusers. We then review some general characteristics of discharges into stationary waters, first for single dense jets, then multiport diffusers with conventional designs and rosettes along with some guidelines for their design. Then some effects of flowing currents are discussed. We conclude with some discussion of mathematical modeling and some unresolved and future research issues.

17.2 Environmental Criteria

The potential environmental impacts of concentrate disposal have been discussed in many publications, such as Lattemann and Höpner (2008). They include concentrate and chemical discharges to the marine environment, air pollutants and energy usage. In this chapter, we are only concerned with the design of diffusers whose objective is rapid dilution and mixing. Criteria that have been adopted around the world for such discharges were recently reviewed for the proposed revision to the California Ocean Plan by Roberts et al. (2012) and are summarized in Table 17.1. They mostly involve limitations to salinity in the receiving water that are expressed as, for examples, an absolute level, an absolute increase over background of a few ppt, or an incremental increase of a few percent. These limits are to be met at the edge of a mixing zone, typically defined as extending a few tens or hundreds of meters from the source.

What are the implications of these regulations for diffuser design? The average salinity in the world's oceans is about 35 ppt, somewhat lower in areas of high freshwater input, and higher in areas of high evaporation and low precipitation such as the Gulf of Arabia. So an increment of 1 ppt over background would correspond to an increase of about 3 %. Typical recovery rates for reverse osmosis (RO) plants are of order 50 %, i.e. concentrate and potable water are produced in roughly equal quantities, so the salinity of the concentrate is doubled to about 70 ppt. For this case (50 % recovery, concentrate salinity twice the background level), the dilution required is directly related to the allowable percentage increase over background by:

Table 17.1 International brine discharge regulations (after Roberts et al. 2012)

Region/Authority	Salinity Limit	Compliance point (relative to discharge)
US EPA	Increment ≤ 4 ppt	–
Carlsbad, CA	Absolute ≤ 40 ppt	1,000 ft (304.8 m)
Huntington Beach, CA	Absolute ≤ 40 ppt salinity (expressed as discharge dilution ratio of 7.5:1)	1,000 ft (304.8 m)
Western Australia guidelines	Increment < 5 %	–
Oakajee Port, Western Australia	Increment ≤ 1 ppt	–
Perth, Australia/ Western Australia EPA	Increment ≤ 1.2 ppt at 50 m and ≤ 0.8 ppt at 1,000 m	50 m and 1,000 m
Sydney, Australia	Increment ≤ 1 ppt	50-75 m
Gold Coast, Australia	Increment ≤ 2 ppt	120 m
Okinawa, Japan	Increment ≤ 1 ppt	Mixing zone boundary
Abu Dhabi	Increment ≤ 5 %	Mixing zone boundary
Oman	Increment ≤ 2 ppt	300 m

$$S = \frac{100}{PC} = \frac{c_b}{c - c_b} \quad (17.1)$$

where S is the required dilution, PC the allowable percentage increase over background, c_b the ambient salinity and c the concentrate salinity. For example, an increment of 3 % requires a dilution of 33:1, an increment of 5 % a dilution of 20:1, etc. These dilutions can be readily achieved by a diffuser with high velocity jets, as discussed below.

17.3 Experimental Techniques

In the following sections we will rely heavily on laboratory experimental studies of dense jets in various flow situations. Such studies have formed the basis for much of our knowledge of the dynamics of dense jets and for diffuser design. They are also essential in validating and developing mathematical models of jet behavior. Visualization of flows can be as simple as adding dye to the discharges, or, more recently, by laser-induced fluorescence (LIF) dye techniques.

We will extensively use images obtained by LIF laboratory experiments to illustrate the mixing processes. In this technique, a fluorescent tracer dye is added to the flow and a laser causes the dye to fluoresce and emit light that is captured by a camera. By suitable calibration, quantitative tracer concentrations can be obtained from the images. It is beyond the scope of this chapter to describe this technique in detail, but descriptions are given in many publications, for example, Koochesfahani and Dimotakis (1985) and Crimaldi (2008).

In particular, we will show many three-dimensional LIF (3DLIF) images. In this technique a laser sheet is swept horizontally at high speed through the flow and sequential LIF images captured. The images are converted to tracer concentrations (and therefore dilution) and visualized to show three-dimensional distributions by computer graphics methods. The images can also be color-coded to show the concentration (and therefore dilution) distributions in the flows. For a discussion of the 3DLIF method used, see Tian and Roberts (2003).

17.4 Mixing of Single Dense Jets

17.4.1 Analysis

The main flow characteristics for a single dense jet in a stationary environment are shown in Fig. 17.1. The negative buoyancy of the jet causes it to reach a terminal rise height and then falls back to the lower boundary where it spreads as a density current. Vertical jets fall back onto themselves when discharged into a stationary

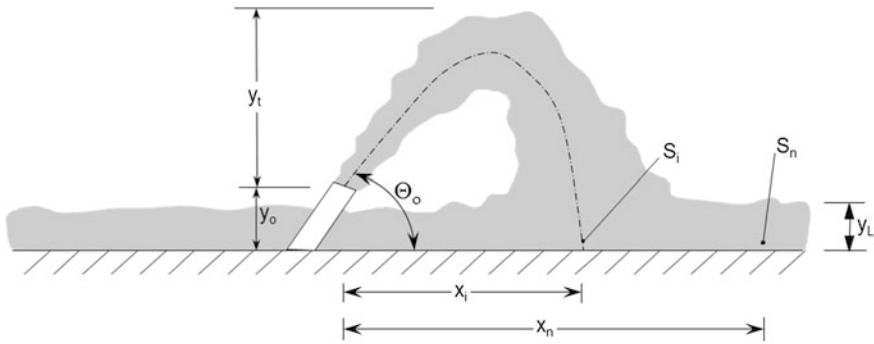


Fig. 17.1 Definition diagram for single dense jet

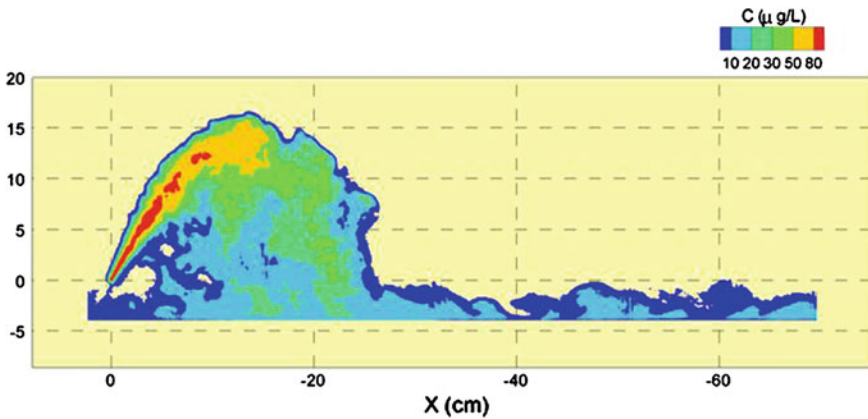


Fig. 17.2 Laser-induced fluorescence (LIF) image of a typical dense jet

environment, resulting in lowered dilutions, so inclined jets are more commonly used. A 60° nozzle inclination seems to have been adopted as the de facto standard for diffuser designs.

These essential flow processes are illustrated by the laser-induced fluorescence (LIF) image through the vertical central plane of a typical 60° dense jet shown in Fig. 17.2. The jet first ascends to a terminal rise height. As it rises, it entrains ambient water that mixes with and dilutes the discharges so that tracer concentrations (and therefore effluent salinity) decrease. It then begins to descend back to the floor, continuing to entrain and dilute as it falls. After impact it spreads horizontally as a density current which is still turbulent and thereby entrains more flow resulting in further dilution. This turbulence eventually collapses under the influence of its own density stratification, marking the end of the near field. The dilution at the end of the near field can be considerably higher than that at the initial jet impact point.

The analysis of this flow is well known, e.g. Roberts et al. (1997). The jet is primarily characterized by its kinematic fluxes of volume, Q , momentum, M , and buoyancy, B ,

$$Q = \frac{\pi}{4}d^2u; \quad M = uQ; \quad B = g'_0Q \quad (17.2)$$

where d is the port diameter, u the jet exit velocity, $g'_0 = g(\rho_a - \rho_0)/\rho_0$, is the modified acceleration due to gravity, g the acceleration due to gravity, ρ_a the ambient density and ρ_0 the effluent density ($\rho_0 > \rho_a$).

As discussed in many publications, the most important length-scale of the flow is $l_m = M^{3/4}/B^{1/2}$ although this is essentially equal to and more commonly expressed as dF where F is the jet densimetric Froude number:

$$F = \frac{u}{\sqrt{g'_0d}} \quad (17.3)$$

If the Froude number is greater than about 20, the volume flux Q is not dynamically significant (or, equivalently, the nozzle diameter is not an important length scale of the flow). For that case any dependent variable, such as the terminal rise height y_t , is a function of M and B only:

$$y_t = f(M, B) \quad (17.4)$$

which, following a dimensional analysis leads to:

$$\frac{y_t}{dF} = \text{Constant} \quad (17.5)$$

Similar analyses lead to the following expressions for the other major jet geometric parameters:

$$\frac{y_t}{dF} = 2.2; \quad \frac{x_i}{dF} = 2.4; \quad \frac{x_n}{dF} = 9.0; \quad \frac{y_L}{dF} = 0.7 \quad (17.6)$$

and for dilution:

$$\frac{S_i}{F} = 1.6; \quad \frac{S_n}{F} = 2.6 \quad (17.7)$$

where the values of the constants are taken from Roberts et al. (1997). The variables in Eqs. 17.6 and 17.7 are defined in Fig. 17.1: y_t is the terminal rise height, x_i the location of the jet impact point (and location of the minimum dilution on the lower boundary), x_n the length of the near field, y_L the thickness of the spreading layer, S_i the dilution at the impact point, and S_n the near field dilution (termed the ultimate dilution in Roberts et al. 1997). Equations 17.6 and 17.7 apply when the jets are fully turbulent, i.e. the jet Reynolds number, $Re = ud/\nu$ where ν is the kinematic

fluid viscosity is greater than about 2000, and the Froude number is greater than about 20, when the dynamical effect of the source volume flux becomes negligible. These conditions will be satisfied by the jets issuing from typical concentrate diffusers.

17.4.2 Effect of Water Depth

The results summarized above are applicable when the receiving water depth is much greater than the jet rise height so there is no interaction with the free surface. It is sometimes necessary to situate diffusers in shallow water, however, where the jets may interact with the water surface, modifying their flow dynamics and possibly reducing dilution.

This introduces another parameter: the water depth, H , and a dimensionless parameter, dF/H that determines its effect. If $dF/H \ll 1$ the flow is fully submerged and Eqs. 17.6 and 17.7 would be expected to apply. If $dF/H \gg 1$ the flow is strongly affected by the water surface.

Jiang et al. (2012) measured the minimum surface dilution for various water depths and delineated three flow regimes: deep water where the jet is unaffected by the water surface, surface contact where the top of the jet impacts the water surface, and shallow water where the jet centerline intersects the water surface. Jiang et al. (2014) extended this study by investigating flow trajectory, cross-sectional profiles, and surface and return point dilutions for 30° and 45° dense jets in limited depths.

Abessi and Roberts (2014c) report further 3DLIF experiments. The experiments were conducted with nozzles oriented at 30°, 45°, and 60°. Typical 3DLIF flow images of a 60° jet in shallow water are shown in Fig. 17.3. They reveal complex three-dimensional interactions with the free surface, especially for steep nozzle angles in the shallow water regime. Time-averaged concentration fields were extracted from the central planes and used to measure the major flow characteristics: Dilutions at the maximum rise height, bottom impact point, and near field, and their locations. Normalized expressions for each parameter were derived and plotted versus dF/H .

For the deep water condition, the results followed those previously reported for fully submerged jets. As the depth decreases the top of the jet begins to interact with the water surface. This occurs at $dF/H = 0.82, 0.52, \text{ and } 0.44$ for nozzle angles of 30°, 45°, and 60°, respectively. As the depth decreases further dilution decreases and eventually the jet centerline intersects the water surface marking the transition to the shallow water regime. This occurs at $dF/H = 1.4, 0.8, \text{ and } 0.78$ for nozzle angles of 30°, 45°, and 60°, respectively. Tracer concentration profiles in the surface contact region are truncated by the water surface and are unsymmetrical. In the shallow water regime they resemble half-Gaussian profiles similar to those of wall

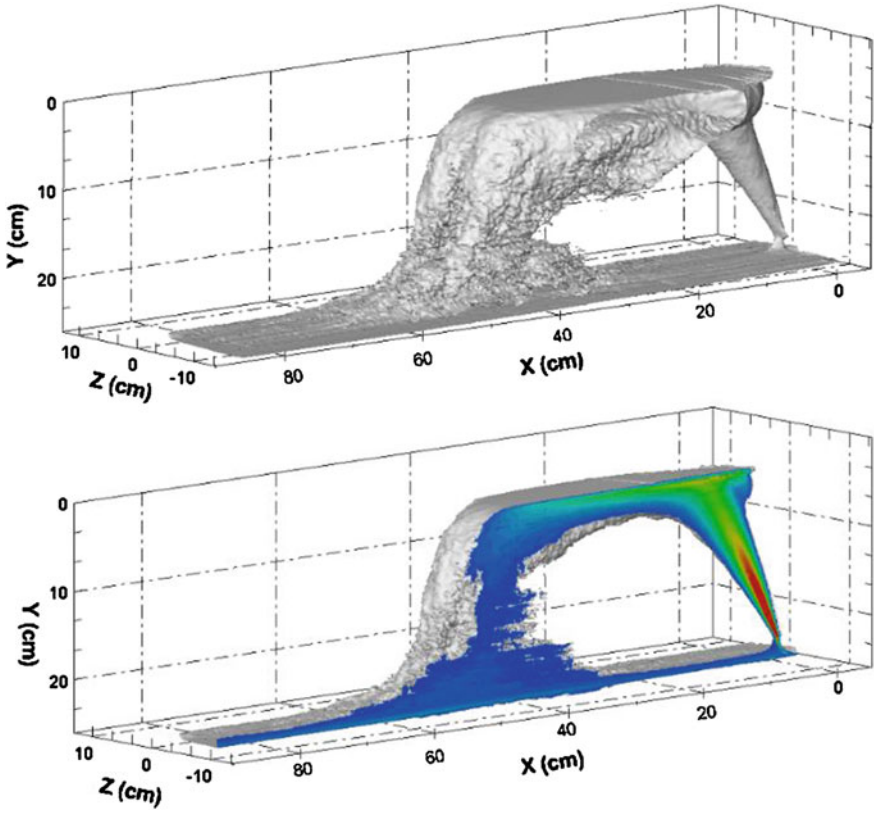


Fig. 17.3 3DLIF image of 60° dense jet in shallow water (from Roberts and Abessi 2014)

jets. The jets can cling to the water surface, although the locations of the bottom impact point and near field lengths are not significantly affected. The complex three-dimensional flows that can result with surface interactions may make them challenging to predict with mathematical models.

Of most importance for design are dilutions at the impact point and near field. In the deep water and surface contact regimes 60° nozzles gave the highest dilutions, as found in previous studies. As the depth decreases, however, the dilutions of the three nozzle angles become more similar, until for shallow water the 30° nozzle gives somewhat higher dilution. If it is necessary to situate a diffuser in shallow water, there may be advantages to the 30° nozzle because of its higher dilution and because there is less surface interaction and visual impact on the water surface.

17.5 Multiport Diffusers

17.5.1 Introduction

Most studies of the dynamics and mixing of inclined dense jets have been with single jets, but multiport diffusers have also been used and are becoming more common. Examples are Perth, Sydney, and Melbourne, Australia. Most designs have been based on formulae derived from experiments conducted with single jets. In a multiport diffuser the nozzles may discharge perpendicular to the diffuser axis and be uniformly distributed along either one or both sides of the diffuser. Or the nozzles may be clustered in rosettes each having multiple ports. The Perth diffuser has 40 ports distributed uniformly along one side of the diffuser at four meter intervals (Marti et al. 2011); the Sydney diffuser has two rosette risers spaced 25 m apart, each riser has four ports. Some hydraulic model tests of specific multiport diffusers have been made, for example Tarrade and Miller (2010).

Systematic studies of the effect of port spacing have been recently reported by Abessi and Roberts (2014a) to obtain guidelines to aid in the rational design of multiport diffusers. Their experiments were conducted on multiport diffusers that discharge from one or both sides and with rosette diffusers. The experiments were conducted with and without ambient currents and the various discharge parameters were systematically varied to cover a range expected for typical ocean outfall diffusers. Below we discuss some results of the studies on multiport diffusers with zero current. The experiments on multiport diffusers in flowing currents and on rosettes are discussed later.

17.5.2 Analysis

Consider the multiport diffuser shown in Fig. 17.4 (with discharge either from one or both sides) whose port spacing is s . For this case, the constants on the right hand sides of Eqs. 17.6 and 17.7 then become functions of s/dF :

$$\frac{y_t}{dF} = f\left(\frac{s}{dF}\right); \quad \frac{x_i}{dF} = f\left(\frac{s}{dF}\right); \quad \frac{x_n}{dF} = f\left(\frac{s}{dF}\right); \quad \frac{S_i}{F} = f\left(\frac{s}{dF}\right); \quad \frac{S_n}{F} = f\left(\frac{s}{dF}\right) \quad (17.8)$$

The effect of the port spacing is therefore entirely encapsulated in the dimensionless parameter s/dF .

Equation 17.8 has two asymptotic solutions. For $s/dF \gg 1$ the ports are widely spaced and the jets do not interfere so the solutions should approach those for a single jet, Eqs. 17.6 and 17.7. For $s/dF \ll 1$, the jets are close together and may behave as if emitted from a line, or slot, source. In that case, the relevant discharge parameters are not the individual jet momentum and buoyancy fluxes, but the volume, momentum, and buoyancy fluxes per unit diffuser length: q , m , and b :

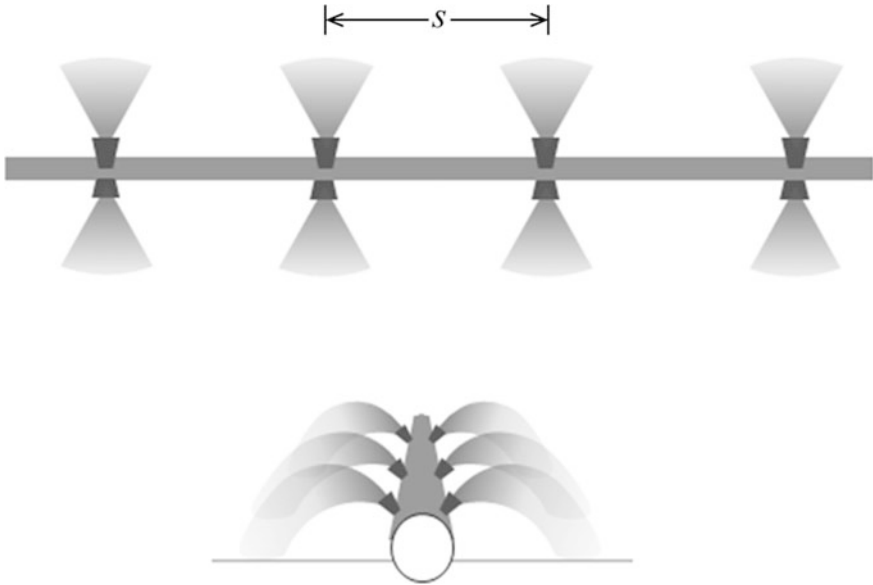


Fig. 17.4 Definition sketch for multipoint dense effluent diffuser (from Roberts and Abessi 2014)

$$q = \frac{Q_T}{L}; \quad m = uq; \quad b = g'_0 q \quad (17.9)$$

where Q_T is the total discharge from the diffuser and L the diffuser length. The analysis analogous to Eq. 17.4 for a line source is then:

$$y_i = f(m, b) \quad (17.10)$$

which, following a dimensional analysis becomes:

$$\frac{y_i b^{2/3}}{m} = \text{Constant} \quad (17.11)$$

For a long diffuser $b = B/s$ and $m = M/s$ and it can be shown that Eq. 17.11 becomes, after some manipulation, and using the definition of the Froude number, Eq. 17.3:

$$\frac{y_i}{dF} = C_1 \left(\frac{s}{dF} \right)^{-1/3} \quad (17.12)$$

Similar arguments apply to the other geometrical parameters, and for dilution:

$$\frac{S_n}{F} = C_6 \left(\frac{s}{dF} \right)^{1/3} \tag{17.13}$$

where C_I and C_6 are experimental constants. These equations should apply to diffusers with discharges from one or both sides, although the values of the constants may differ. As the jets are moved closer together, Eq. 17.12 implies that the rise height increases and Eq. 17.13 implies that the dilution decreases.

We would expect a transition between the single jet solutions ($s/dF \gg 1$) and line jet solutions ($s/dF \ll 1$) to occur at $s/dF \sim O(1)$. Systematic experiments were performed to test these hypotheses and to investigate the nature of these relationships.

The results for near field dilution are shown in Fig. 17.5; for other results see Abbessi and Roberts (2014a).

The results follow the expected point-source asymptotic solutions for $s/dF > \sim 2$ but for smaller spacings they do not follow the expected line source solutions. The rise height actually decreases as the spacing decreases rather than increases as predicted by Eq. 17.12. The impact and near field dilutions do decrease with spacing as expected, but much more rapidly than predicted by Eq. 17.13.

The following empirical equations were fitted to the results for $s/dF < \sim 2$:

$$\frac{y_t}{dF} = 1.9 \left(\frac{s}{dF} \right)^{1/2}; \quad \frac{x_i}{dF} = 2.0 \left(\frac{s}{dF} \right)^{1/2}; \quad \frac{x_n}{dF} = 6.0 \left(\frac{s}{dF} \right)^{1/2} \tag{17.14}$$

$$\frac{S_i}{F} = 0.9 \left(\frac{s}{dF} \right); \quad \frac{S_n}{F} = 1.1 \left(\frac{s}{dF} \right) \tag{17.15}$$

where the values of the constants are for diffusers discharging from one side.

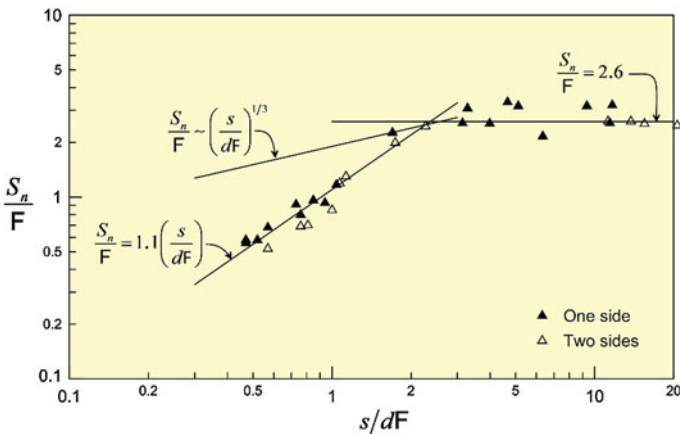


Fig. 17.5 Near field dilution of multiport dense effluent diffuser (from Roberts and Abbessi 2014)

Even allowing for experimental scatter, Fig. 17.5 indicates that dilutions for diffusers with ports on both sides are systematically lower by about 20 % than for diffusers discharging to one side only (for otherwise similar values of F and s/dF). This reduction appears to be real despite the wide separation between the flows from each side (for example, Fig. 17.6). It is a secondary effect, probably mainly due to the slightly thicker bottom layer that forms with a discharge from both sides (which doubles the total discharge per unit diffuser length), thereby slightly increasing re-entrainment into the falling jet near the lower boundary. The corresponding constants for dilution for two-sided discharges would therefore be about 20 % lower than those given in Eq. 17.15.

Why the results did not follow those predicted for slot jets became evident from animations of the flows beginning at initiation of discharge. The jets at first rose much higher and then their rise height decreased to approach those shown in Fig. 17.6. The falling jets were re-entrained by the rising jets, filling the cavity between them and impeding their upward motion. The entrained flow could not penetrate through the jets to the interior, starving them and reducing dilution. This “sucking in” of the jets shortened the jet impact point distance and the length of the near field compared to similar single jets. This effect is also known as the Coanda effect. Clearly, the spacing must be large enough that entraining flow is freely available for the jets. According to Fig. 17.5 this occurs when $s/dF > \sim 2$.

These results are generally consistent with the model studies that have been reported for multiport diffusers such as Miller et al. (2006). They are also consistent with the field observations for full flow of the Perth Stage 1 diffuser (discharge from

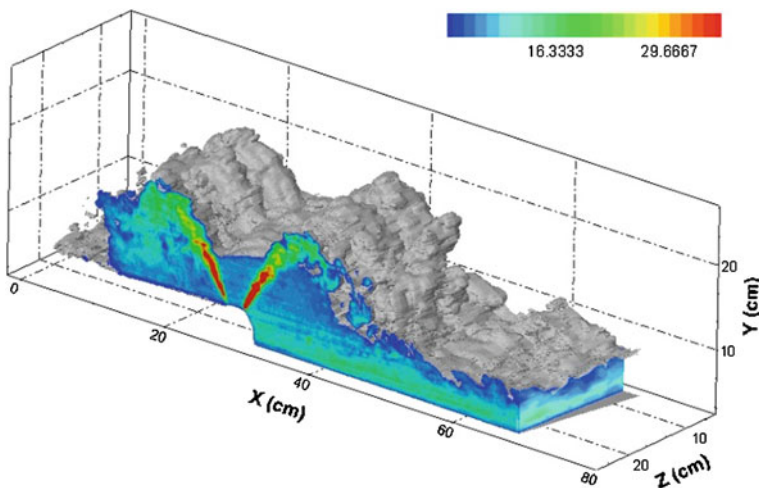


Fig. 17.6 3DLIF “instantaneous” image of flow from a multiport diffuser. $F = 46$, $s/(dF) = 0.6$ (from Roberts and Abessi 2014)

one side) reported by Marti et al. (2011) correspond to $s/dF \sim 1.3$, which is in the transition for port spacing effect.

Coanda dynamical interaction between buoyant jets from multiport diffusers can be important and has been noted in several contexts. It arises from the “Bernoulli” effect whereby proximity to a boundary or jet changes the entrained flow pattern resulting in a pressure force that deflects the jet towards it. If there is a boundary, such as the bed or water surface, the jet can cling to it; if there are adjacent jets, they entrain each other. An example for positively buoyant jets can be seen in Fig. 1a of Roberts et al. (1989). In the central region, the pressure force (or entrainment flow) is equally balanced on each side of the plumes and they rise vertically. The end plumes bend inwards, however, due to the unbalanced inward force acting on them.

Lai and Lee (2012) considered the dynamical interaction between multiple buoyant jets due to the induced pressure field. To predict the flow and pressure distribution they assume that the entrainment is due to distributed point sinks along the jet trajectory (the Distributed Entrainment Sink Approach, DESA, Choi and Lee 2007) and that the induced entrainment field is irrotational. The jet trajectories are then solved iteratively until a steady-state is achieved and the velocity and concentration fields are obtained by superposition. Although not specifically intended for dense jets with self-interaction between their rising and falling phases, this analysis may be applicable.

Similar dynamic interactions have also been noted for rosette diffusers with positively buoyant discharges. Roberts and Snyder (1993) found that increasing the number of ports per riser from 8 to 12 *decreased* dilution due to an inward bending of the plumes that resulted in merging and inhibited entrainment into the plumes’ inner surfaces. Kwon and Seo (2005) also investigated rosette risers with four ports and reported inward bending due to “under pressure” in the flow core. These effects were further investigated in Tian and Roberts (2011) where rosette and “conventional” multiport diffusers were compared. Rosettes with eight ports resulted in inward bending of the plumes due to dynamic interaction, but did not significantly reduce dilution—provided the spacing is wide enough, which it is in the case of eight ports per riser but not twelve. It was also noted that the effect of dynamic interaction is more pronounced with zero currents and becomes less important in flowing currents.

This impaired dilution for merging dense jets is exacerbated by restricted entrainment at the diffuser ends. In the Abessi and Roberts’ experiments, the channel walls are assumed to be planes of symmetry between ports, so the experiments represent the central section of a very long diffuser. For a diffuser of finite length, entrained flow can enter the inner core from its ends. For a single jet (or widely spaced jets) this issue does not arise as entrained flow is freely available, and any re-entrainment in the falling jet is already included in the dimensional analysis. The results of Fig. 17.4 are therefore probably conservative, and actual finite length diffusers should have higher dilutions.

These observations have significant implications for numerical modeling of multiport diffusers for dense jets. Integral entrainment models assume an unrestricted supply of entrainment water, neglect re-entrainment, and neglect dynamical

interaction (Coanda effect) between jets. All of these conditions are violated for the merged jets observed here and integral models may considerably overestimate dilutions. These deficiencies of entrainment models may be alleviated by including dynamic interaction such as by the DESA approach. CFD computations would also be very challenging as the entire flow field and restricted entrainment must be modeled. Physical modeling may be needed to predict these effects for complex diffuser geometries with multiple jets, for example, Miller and Tarrade (2010) and Tarrade and Miller (2010).

The increase in dilution from the impact point to the end of the near field is about 60 % for non-merged jets and 20 % for merged jets. For non-merged jets, that is similar to the observations on single dense jets in Roberts et al. (1997). No previous results have been reported for merged jets, but the increase in dilution from the impact point to the near field for positively buoyant fully merged (line plume) discharges was reported by Tian et al. (2004) to be also about 20 %. Point discharges show more increase because the bottom layer spreads in three dimensions approximately radially with ring-shaped entraining vortices whereas merged jets spread with entraining vortices that are more two dimensional.

In conclusion, for $s/dF > \sim 2$ the jets do not merge and the geometrical and dilution results followed the expected asymptotic results for single jets. For $s/dF < \sim 2$ the jets merged, but did not follow the expected line source solutions. The dilutions decreased as the spacing decreased, as expected, but much more rapidly than predicted. In order to prevent the reduction in dilution due to restricted entrainment, the jets must be sufficiently separated. To accomplish this it is recommended to maintain $s/dF > \sim 2$.

17.6 Rosette Diffusers

Brine outfalls are frequently constructed as tunnels that discharge through risers. As risers and tunnels are expensive to construct, it is desirable to minimize the number of risers and the diffuser length by putting more ports on each riser and minimizing their spacing.

Rosette diffusers with dense discharges also show dynamic jet interactions. In stationary flows, Miller and Tarrade (2010) reported that risers with six ports had lower dilution than with four ports as the jets competed for clear water to entrain. With six risers the entrainment was primarily from above, and dilution was reduced if the tops of the jets were close to the water surface. Of course, there is a fundamental difference between rosettes with positively buoyant discharges compared to those with negatively buoyant discharges. Negatively buoyant flows allow entrainment from the top, as observed by Miller and Tarrade, whereas positively buoyant flows form a horizontal spreading layer that caps off the top. In that case the entraining flow can only come from gaps between the jets.

In a stationary environment, the dilution equation corresponding to Eq. 17.8 is:

$$\frac{S_n}{F} = f\left(\frac{s_r}{dF}\right) \tag{17.16}$$

where s_r is the riser spacing. Experiments to investigate the effect of s_r/dF were conducted by Roberts and Abessi (2014a) using single and multiple risers each containing four ports. Two different riser configurations were studied, as shown in Fig. 17.7. Each had four ports uniformly distributed around the perimeter (i.e. at 90° to each other in planform). The risers were rotated so that the ports were either perpendicular or parallel to the diffuser axis (Fig. 17.7a) or at 45° to the diffuser axis (Fig. 17.7b).

A typical 3DLIF image of a single rosette is shown in Fig. 17.8. Also shown is the concentration distribution along a central plane through two of the jets. The jets are similar to isolated ones although their dilution is somewhat reduced.

Results for near field dilution are shown in Fig. 17.9 along with results for an equivalent conventional diffuser that is assumed to have two ports per riser (in which case the equivalent port spacing is $s = s_r/2$). As for the multiport diffuser, the results become independent of riser spacing when $s_r/dF \gg 1$, in this case greater than about 2.5. The asymptotic value of dilution is less than that for a comparable conventional diffuser, however, because the jets interact even when the risers are widely separated (Fig. 17.8). Conversely, Fig. 17.9 shows that as the risers are moved closer together the dilution for a rosette is greater than that for equivalent two-port risers.

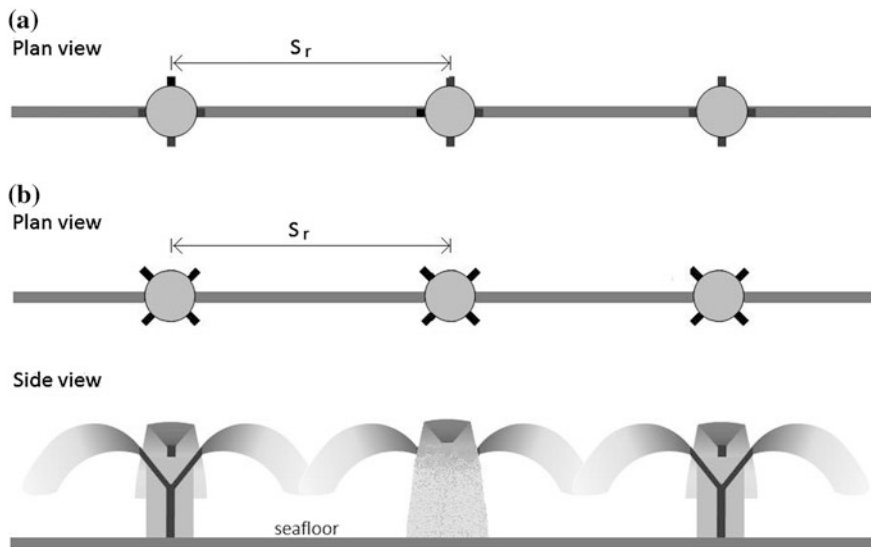


Fig. 17.7 Riser configurations tested (from Roberts and Abessi 2014)

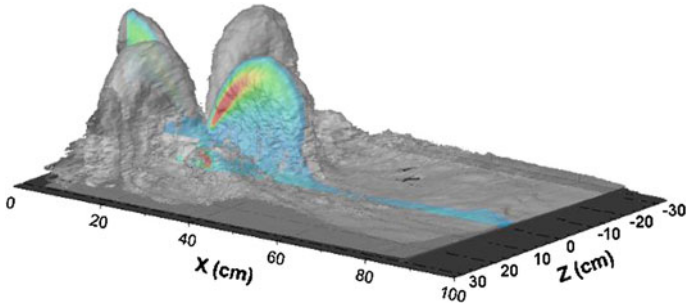
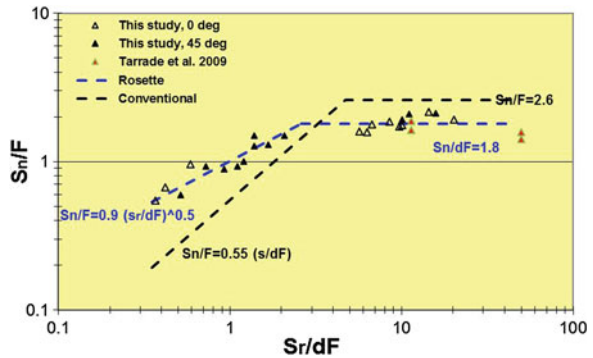


Fig. 17.8 3DLIF single rosette (from Roberts and Abessi 2014)

Fig. 17.9 Effect of riser spacing on near field dilution for 4-port rosettes (from Roberts and Abessi 2014)



The reason for this can be seen in Fig. 17.10 which compares images of a four-port riser and a two-port riser with approximately equal equivalent port spacings ($s_r/dF = 1.5$ for the four-port riser and $s_r/dF = 0.76$ for the two-port riser). As previously discussed, the two-port riser results in merging and restricted entrainment, significantly reducing dilution. The jets from the rosettes, however, remain distinct and able to entrain freely.

17.7 Effects of Flowing Currents

17.7.1 Introduction

The above discussions have been concerned with discharges into stationary environments. This is usually considered to be the worst case for dilution and is the usual basis for design. The ocean is rarely stationary, however, and, with a few notable exceptions, dilution generally increases with current speed. In this section we consider some aspects of the effects of flowing currents.

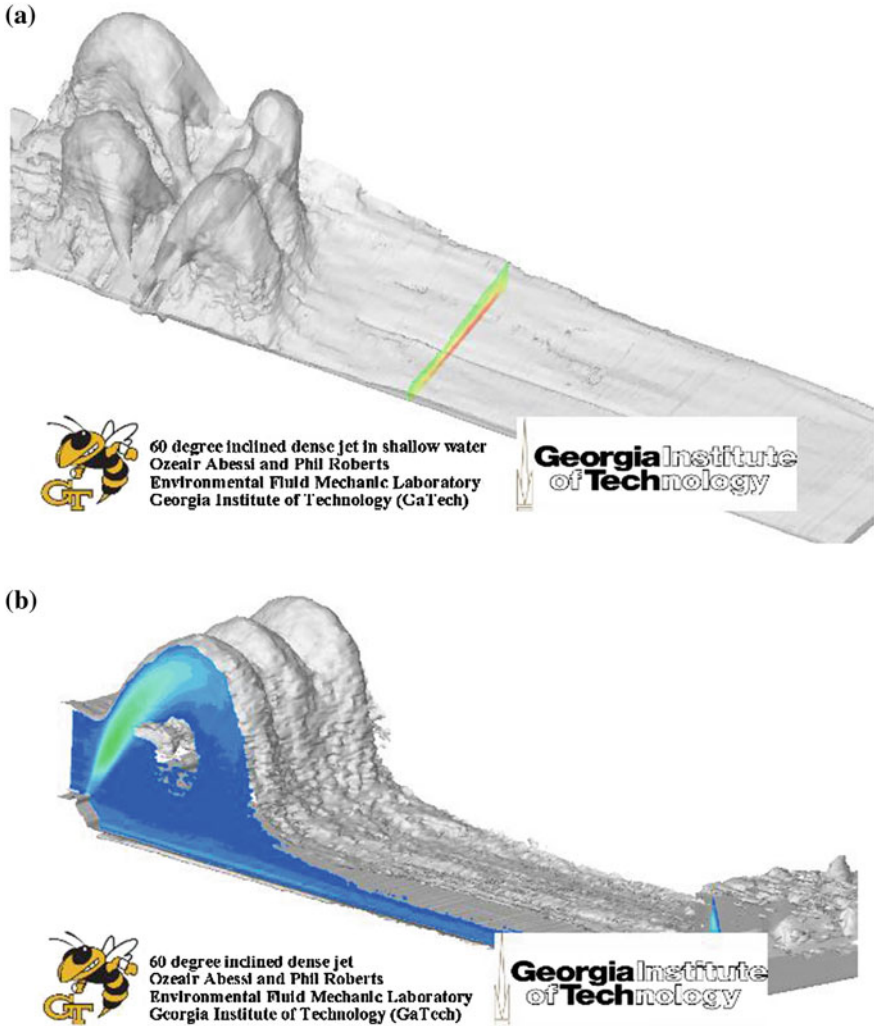


Fig. 17.10 Rosette and conventional diffusers with equivalent port spacings. **a** $S/dF = 1.5$ and **b** $s/dF = 0.76$ (from Roberts and Abessi 2014)

17.7.2 Single Vertical Jet

The simplest case, because it introduces only one new parameter, is the single vertical jet. The new parameter is the current speed, and because the jet is vertical its direction is immaterial.

The dynamical effect of the ambient current is mainly determined (Gungor and Roberts 2009) by the parameter $u_r F$ where $u_r = u_c/u$ is the ratio of the current velocity u_c to the jet velocity u . Note that $u_r F = u_c/\sqrt{g_0 d}$, which is itself a type of

Froude number based on the cross flow velocity, does not contain the jet velocity, u as a parameter. For $u_r F \ll 1$, the current does not significantly affect the jet; the flow characteristics change as $u_r F$ increases, however, as discussed below.

The terminal rise height y_t , the thickness of the bottom layer y_L , and the minimum dilutions at the impact point S_i , and at the terminal rise height S_r , can be written as:

$$\frac{y_t}{dF}, \frac{y_L}{dF}, \frac{S_i}{F}, \frac{S_r}{F} = f(u_r F) \quad (17.17)$$

3DLIF Experiments on vertical dense jets to investigate the form of these equations are reported by Gungor and Roberts (2009).

Based on their studies, the following characteristics of a vertical dense jet in a cross flow emerge as sketched in Fig. 17.11. For zero current speed, the jet reaches a height $y_t \approx 2.2dF$ and then falls back on itself, impairing dilution. This flow is sometimes called a fountain. The bottom layer flows radially in all directions as a density current and mixing continues in this layer beyond the impact point. With a current, the jet is bent downstream, and when $u_r F \geq 0.2$ the ascending and descending parts of the flow separate. Because the ascending flow is now little influenced by the descending flow, the rise height increases and the dilution is higher than with no current. The bottom flow still intrudes as an upstream wedge against the current.

As the current speed increases further, the wedge becomes arrested and cannot propagate upstream. This occurs for a value of $u_r F$ that lies somewhere between 0.24 and 0.37. The rise height is essentially constant over the range $0.2 < u_r F < 0.8$. As $u_r F$ is increased beyond 0.5, the rise height decreases slowly with increasing current speed, the jet is further bent over and impacts the lower boundary farther downstream. The trajectory of the ascending portion of the flow is generally quite steep, almost vertical, and the descending slope much more gradual. Further mixing still occurs in the bottom spreading layer, although it seems to be reduced compared to slower currents. For $u_r F$ greater than about 1, the jet is significantly bent over and it becomes almost horizontal for $u_r F$ greater than about 2. For this case, the jet will probably be dispersed by ambient turbulence in the receiving waters (Pincince and List 1973), i.e. it will go rapidly into the “far field,” and/or be trapped by ambient density stratification. In either case, any impacts of the effluent on the seabed should

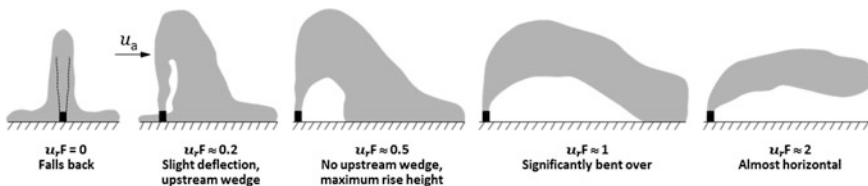


Fig. 17.11 Effect of currents on vertical dense jets (from Gungor and Roberts 2009)

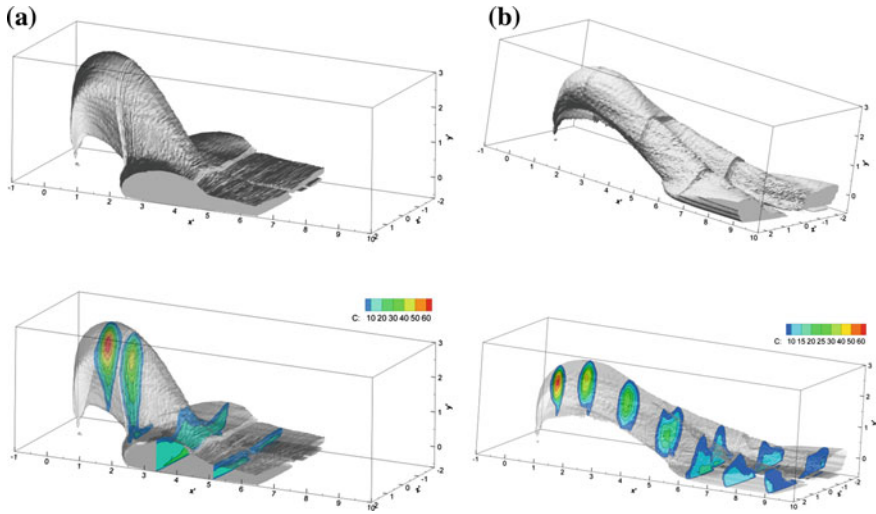


Fig. 17.12 3DLIF images of vertical jets in cross flows (from Gungor and Roberts 2009)

be minimal. The critical speeds of major interest are therefore $u_r F < 1$, which was the range investigated.

Some typical results for a moderate ($u_r F = 0.50$) and strong ($u_r F = 0.9$) currents are shown in Fig. 17.12.

For $u_r F \sim 0.5$, the cross-sectional profiles of tracer concentration are neither axially symmetric nor self-similar. The jet is much taller than it is wide, and the peak concentration occurs much closer to the top. This results from a “gravitational instability” that causes fluid in the lower half of the jet to travel almost vertically and detrain from the jet. The detrained flow can be re-entrained back into the rising jet.

As the current speed increases to $u_r F \sim 0.9$ this asymmetry decreases but other flow phenomena occur. The profiles in the rising portion are approximately radially symmetric but in the falling portion they develop a kidney shape due to formation of two counter-rotating vortices. These vortices cause the jet to almost completely bifurcate after impacting the bottom.

It was found that the rise height was essentially constant over the range of current speeds tested. The distance of the impact point and dilutions at the terminal rise height and impact point increased with current speed. The near field dilution is greater than the impact dilution due to additional mixing in the bottom layer.

The complexity of the flows and the different phenomena that dominate at different locations within the same jet and at different current speeds indicate that predicting these flows numerically will be quite challenging. Entrainment models are often used, but the experiments show flow features that violate some of their fundamental assumptions such as self and radial symmetry, and they also ignore mixing due to gravitational instability. Although entrainment models may predict trajectories reasonably well, their predictions of dilution should be viewed with caution.

17.7.3 Multiport Diffusers

Multiport diffusers in flowing currents involve more parameters than a single vertical jet. The discharge may be from one side of the diffuser only (e.g. Perth) in which case the current may be either co-flowing or counter-flowing relative to the jets, or it may discharge from both sides. Other variables are the port spacing and the angle of the current relative to the diffuser axis. Many experiments on various configurations of multiport diffusers are given in Roberts and Abessi (2014). Here we give just a few examples of the flows that may arise. The effects of port spacing and current are expressed by the dimensionless parameters $u_r F$ and s/dF .

Co-flowing cases are illustrated in Fig. 17.13 which shows typical images for wide and narrow port spacings at various current speeds. The trajectories of a line source ($s/dF \ll 1$) are different from a point source ($s/dF \gg 1$); generally the trajectory is longer for point sources. The rise height decreases as $u_r F$ increases with a break point near $s/dF \approx 0.7$ for most $u_r F$; beyond this point the maximum rise height does not change with s/dF and the flow behaves like a point source. The impact point moves farther downstream as $u_r F$ increases.

Dilution at the maximum rise height and downstream both increase with $u_r F$. For $s/dF > \approx 0.7$ dilution does not change with s/dF and the flow approximates a point source. Impact point dilution increases with $u_r F$ and also with s/dF which indicates that some merging occurs at some point downstream for smaller s/dF .

Counter-flowing cases are illustrated in Fig. 17.14. Again the trajectories differ for line and point sources. The images also show an important phenomenon: at a particular current speed the jet can fall back directly on itself, which leads to reduced dilution. This occurs for $u_r F \approx 0.67$. For higher current speeds, the maximum rise height decreases when $u_r F$ increases.

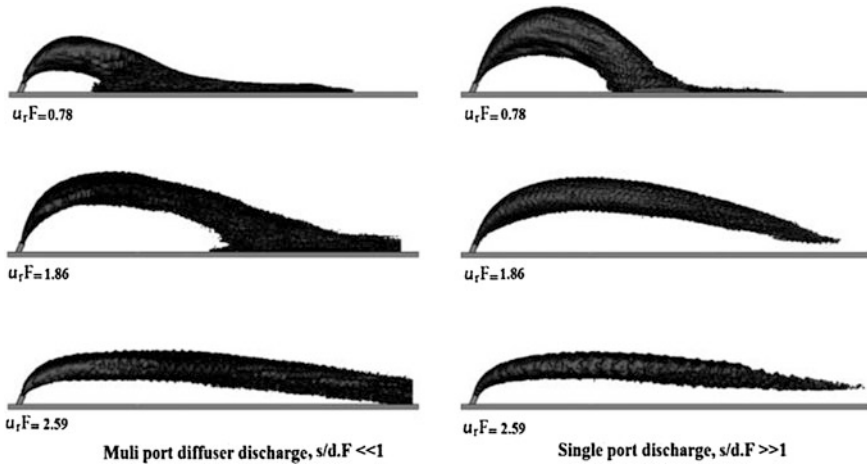


Fig. 17.13 Discharges in co-flowing currents for line sources ($s/dF < 0.62$) and point sources ($s/dF > 1.91$) (from Roberts and Abessi 2014)

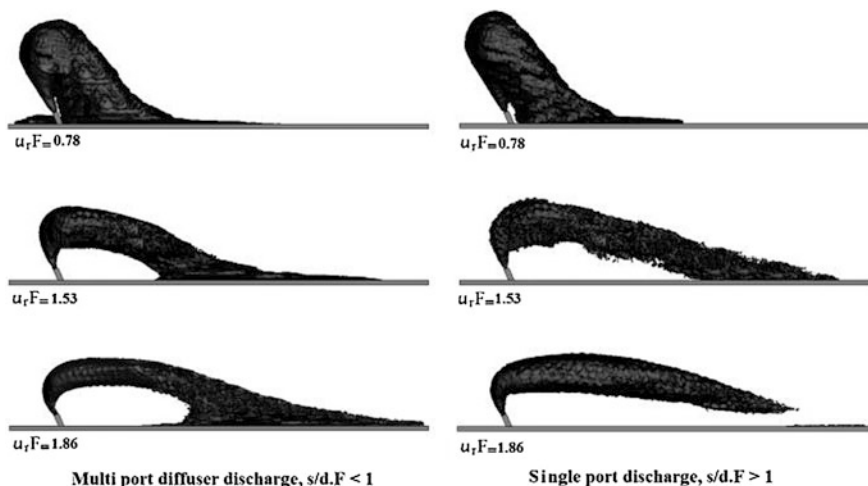


Fig. 17.14 Multiport and single port discharges in counter-flowing current (from Roberts and Abessi 2014)

The maximum rise height and dilution depend on port spacing (s/dF). They increase with s/dF up to $s/dF \approx 0.7$ and then become independent of s/dF when the flows behave like point sources. The jet trajectories are influenced by merging; point source flows impinge the bed farther downstream than do line sources.

Finally, multiport diffusers with flows from both sides are illustrated in Fig. 17.15. Some experiments were conducted with a gap between the diffuser bottom and the channel bed to allow flow underneath the diffuser, and some with no gap. These two conditions are referred to as “blocked” and “unblocked.”

The pattern of merging depends on the port spacing (s/dF) and the current speed ($u_r F$). For narrow spacing, the jets from both sides first merge with their neighbors and then with those from the opposite side of the diffuser. For wide spacing, the jets first merge with their corresponding jets from the opposite side, then with their neighbors. Figure 17.15 shows that the flow field can be significantly impacted by the presence or absence of the gap, which allows flow under the diffuser.

The wastefield geometric characteristics and dilution also depend on s/dF and $u_r F$. The rise height increases with s/dF in the range of 0.9–4.1, but differs for blocked and unblocked flows. The impact location for blocked and unblocked flows does not show any dependence on s/dF , although it is apparently shorter for the unblocked cases. The impact point dilution also increases with s/dF over the range of tested parameters and differs for blocked and unblocked cases. The flow trajectories show a significant influence of blocking; it increases the maximum rise height and decreases the impact point length. The blocked flow dilution at impact is less than when unblocked. These results show how a small gap beneath the diffuser and therefore relatively small changes in diffuser configuration can significantly impact the flow field in moving ambient waters.

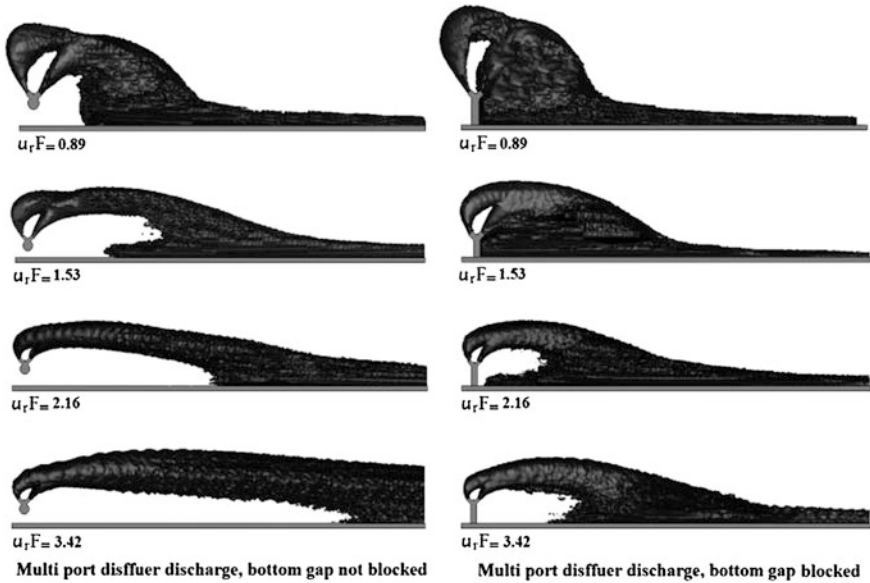


Fig. 17.15 Effect of flow blocking on discharges from multiport diffusers (from Roberts and Abessi 2014)

17.7.4 Rosette Diffusers

Experiments with single and multiple four-port rosettes in flowing currents are also reported in Roberts and Abessi. Again, multiple parameters are involved, including current speed, riser spacing, and rosette rotation (0° and 45°). Here we show just one example in Fig. 17.16. It is for a single riser with 0° rotation.

The four plumes merge downstream to a single one. For multiple risers, depending on the riser spacing, the jets may merge before interacting with those from a neighboring riser, or the jets issuing from adjacent risers may merge first. Examples are presented in Roberts and Abessi where results are given for dilutions and geometrical parameters for various flow conditions. Normalized trajectories for various $u_r F$ show the importance of current on the flow behavior and how increases in ambient cross flow increase the distance of the impact point and dilution at this point. The influence of riser rotation is of secondary importance and can be ignored.

17.8 Mathematical Models

The above discussions have emphasized the physical aspects of near field mixing of dense jets. In many cases, satisfactory diffuser designs can be made by using the semi-empirical equations and “worst-case” conditions such as zero current speeds.

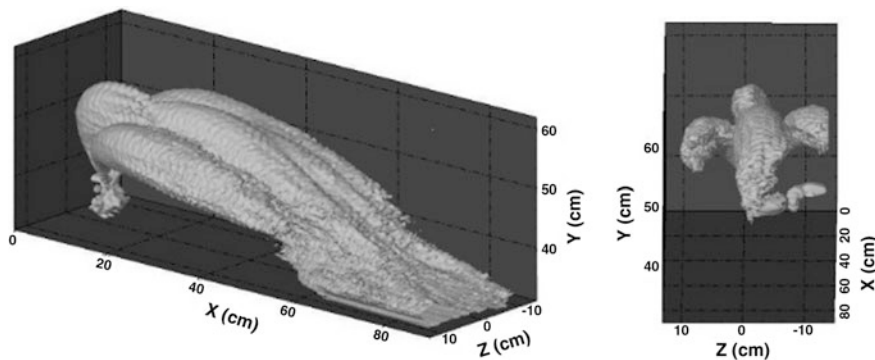


Fig. 17.16 Flow configuration for rosette diffusers in flowing water: 0° orientation (from Roberts and Abessi 2014)

Mathematical models are also essential of course, and means to couple the near field dynamics with far field hydrodynamic models to assess larger scale impacts are needed. Most near field models are of the entrainment, or integral, type or computational fluid dynamics (CFD).

Entrainment models are the most common ones used in engineering to predict near field dynamics of jets and plumes. Although they can be used for dense jets, their limitations should be kept in mind. They assume incorporation of external fluid into the jet by entrainment and the profiles of velocity and tracer concentration to be self-similar and axially symmetric. As shown here, however, dense jet flows often violate these assumptions, leading to unreliable predictions. For example, Pincince and List (1973) concluded that, although jet trajectories were reasonably predicted, dilutions were considerably underestimated. Anderson et al. (1973) concluded that the models can only predict trends, rather than exact dilutions and trajectories.

The vertical asymmetry in the tracer profiles, whereby the peak concentration is closer to the top (similar to Fig. 17.12a), has been observed in many previous studies of dense inclined jets in stationary environments and in cross flows. Lane-Serff et al. (1993) point out that the top half of the jet is gravitationally stable, with density decreasing upwards, but the bottom half is unstable, with heavier fluid above lighter fluid. This leads to the upper plume edge being sharp and well defined, but in the lower half fluid can detrain from the jet so the lower boundary is poorly defined. Lindberg (1994) also noted in his experiments with cross flows that low momentum fluid almost immediately descended after leaving the nozzle and this continued through the jet trajectory, and Kikkert et al. (2007) observed it in stationary inclined jets. This gravitational instability also leads to enhanced mixing within the jet and also between the jet and the environment.

Integral models do not usually include the additional mixing that occurs within the near field beyond jet impact. This can be substantial: for inclined jets in stationary environments, Roberts, et al. (1997) find the increase in dilution between the impact point and the end of the near field to be around 60 %.

Dynamical interaction of merging jets from multiport diffusers result in further complications. As discussed above, the jets entrain, or attract, each other, by the Coanda effect. If they are too close together (Fig. 17.6 for example), the supply of entraining water is restricted resulting in reduced dilution. In general, entrainment models do not predict the Coanda effect, which reduces jet rise height and dilution. For these cases, physical modeling may be more reliable.

Entrainment models may be Lagrangian, for example UM3 in the EPA model suite Visual Plumes, or VISJET, or Eulerian such as CORJET. For a recent extensive discussion and comparison of these models for simulating dense jets in stationary environments, see Palomar et al. (2012a, b). They found significant discrepancies between the models. Differences in dilution rate estimation were significant, motivating further review of the entrainment closure models and simplifying the assumptions made by integral models.

Computational fluid dynamics (CFD) models are now increasingly applied to a wide variety of turbulent flows in nature and engineering. There are several major CFD techniques; for a review, see Sotiropoulos (2005). One method is direct numerical simulation (DNS) where the unsteady, three-dimensional Navier-Stokes equations are solved over scales small enough to resolve the entire turbulence spectrum. The computational resources increase dramatically with Reynolds number, however, so DNS is not yet a practical modeling tool for simulating flows at engineering-relevant Reynolds numbers. Large Eddy Simulation (LES) solves the spatially filtered unsteady Navier-Stokes equations to resolve motions larger than the grid size, and models smaller-scale motions with a sub-grid model. For high Reynolds number flows of practical engineering interest very high grid resolutions and supercomputers are still required however. The most common CFD models are Reynolds-decomposition models. Flow quantities are decomposed into time-averaged and fluctuating values and the Navier-Stokes equations are then time averaged, producing what are known as the Reynolds-averaged Navier-Stokes (RANS) equations. Various adaptations of this model have been applied to many engineering flows.

There have been fewer applications of CFD to jet and plume-type flows. Hwang and Chiang (1995) and Hwang et al. (1995) simulated the initial mixing of a vertical buoyant jet in a density stratified cross flow. Blumberg et al. (1996) and Zhang and Adams (1999) used far-field CFD circulation models to calculate near field dilutions of wastewater outfalls. Law et al. (2002) used a revised buoyancy extended turbulence closure model to investigate the dilution of a merging wastewater plume from a submerged diffuser with 8-port rosette-shaped risers in an oblique current. Davis et al. (2004) used commercial codes to simulate several case studies of effluent discharges into flowing water, including a line diffuser, a deep ocean discharge, and a shallow river discharge. They concluded that CFD models are becoming a viable alternative for diffuser discharges with complex configurations.

The paucity of CFD applications to near field mixing is because of the challenges that they face. These arise from the geometrical complexity of realistic multiport diffusers, the large difference between port sizes and the other characteristic length scales, buoyancy effects, plume merging, flowing current effects, and

surface and bottom interactions. To overcome these difficulties, Tang et al. (2008) applied a three-dimensional RANS model using a domain decomposition method with embedded grids to model diffusers. CFD models of brine discharges have been reported by Muller et al. (2011), Oliver et al. (2008), and Seil and Zhang (2010). Although promising, the complexity of CFD models, the effort required to set them up and long run times suggests that entrainment and length-scale models will continue to be used for many years.

17.9 Concluding Remarks

In this chapter we have attempted to summarize and highlight some of the essential features of dense jets typical of those encountered in brine concentrate diffusers. It is possible to design a diffuser that will effect high initial dilution and safely dispose of concentrate with minimum environmental impacts. We have emphasized the physical aspects using laboratory experiments and visualizations to illustrate these processes. In many cases, the main features such as rise height, layer thickness, and dilution, can be estimated, and designs made, using the simple empirical formulae such as those presented here. More complex situations may require mathematical models. As pointed out, however, modeling is not simple. Entrainment models are frequently used, but they do not readily incorporate some flow features, in particular, lack of radial symmetry, changing flow characteristics along the jet trajectory, internal mixing due to gravitational instability, re-entrainment, dilution in the spreading layer, turbulence collapse and dynamical interaction between multiple jets. CFD models are being increasingly used in hydraulic engineering and their use will certainly increase in the future. They also face challenges, however, in simulating the features mentioned above and also their need to simulate the entire flow field, difficulty of grid and model setup, and long run times. Entrainment models will therefore probably be the mainstay of engineering calculations for some time with dynamical interactions possibly augmented by the DESA approach such as Choi and Lee (2007).

This dynamical interaction and Coanda effects should be acknowledged and incorporated into design, although they are difficult to predict mathematically. Experiments on multiport jets also show that small changes in diffuser design can result in significant changes in the flow field and therefore dilution. The difficulty of predicting these effects may indicate the need for physical models in complex situations.

Although the main features of dense jet dynamics are reasonably well understood, there remain many intriguing questions of a more fundamental research nature. For example, the dynamics of the bottom layer on sloping seabeds. This would probably increase dilution compared to the present results so the horizontal bed should be considered a “worst-case” for dilution. Bed forms could also have an impact.

Boundary interactions with the jet and its effect on dilution can also be important. Abessi and Roberts (2014b) report that as the descending jet approaches the lower boundary dilution tends to a constant value and then actually decreases in a thin boundary layer up to the wall. The presence of this thin layer may explain wide discrepancies in reported dilutions and may be environmentally important due to exposure of benthic organisms to high salinities. It does not persist far from the impact point, however, as it is swept up by the ring-like vortices that propagate radially from the impact point. The vortices entrain ambient fluid and increase dilution but they eventually collapse under their self-induced density stratification, marking the end of the near field. The dynamics of this collapse is not well understood.

Acknowledgments The author wishes to acknowledge and express his appreciation to Dr. Ozeair Abessi for his great expertise in tirelessly running many of the experiments discussed here and for many discussions on the mechanics of complex dense jet dynamics.

References

- Abessi, O., & Roberts, P. J. W. (2014a). Multiport diffusers for dense discharges. *Journal of Hydraulic Engineering*, 140(8).
- Abessi, O., & Roberts, P. J. W. (2014b). Effect of nozzle orientation on dense jets in stagnant environments. *Journal of Hydraulic Engineering* (Submitted).
- Abessi, O., & Roberts, P. J. W. (2014c). Dense jet discharges in shallow water. *Journal of Hydraulic Engineering* (Submitted).
- Blumberg, A. F., Ji, Z.-G., & Ziegler, C. K. (1996). Modeling outfall behavior using far field circulation model. *Journal of Hydraulic Engineering Division of the American Society of Civil Engineers*, 122(11), 610–616.
- Choi, K. W., & Lee, J. H. W. (2007). Distributed entrainment sink approach for modeling mixing and transport in the intermediate field. *Journal of Hydraulic Engineering Division of the American Society of Civil Engineers*, 133(7), 804–815.
- Crimaldi, J. P. (2008). Planar laser induced fluorescence in aqueous flows. *Experiments in Fluids*, 44(6), 851–863.
- Davis, L., Davis, A., & Frick, W. (2004). Computational fluid dynamic application to diffuser mixing zone analysis—Case studies. In *3rd International Conference on Marine Wastewater Disposal MWWDD 2004*, Catania, Italy, September 27–October 2, 2004.
- Gungor, E., & Roberts, P. J. W. (2009). Experimental studies on vertical dense jets in a flowing current. *Journal of Hydraulic Engineering Division of the American Society of Civil Engineers*, 135(11), 935–948.
- Hwang, R. R., & Chiang, T. P. (1995). Numerical simulation of vertical forced plume in a crossflow of stably stratified fluid. *Journal of Fluids Engineering*, 117, 696–705.
- Jiang, B., Law, A. W.-K., & Lee, J. H.-W. (2012). Mixing of 45° inclined dense jets in shallow coastal waters: surface impact dilution. *Third International Symposium on Shallow Flows*, Iowa City, Iowa, USA.
- Jiang, B., Law, A. W.-K., & Lee, J. H.-W. (2014). Mixing of 30° and 45° inclined dense jets in shallow coastal waters. *Journal of Hydraulic Engineering Division of the American Society of Civil Engineers*, 140(3), 241–253.
- Kikkert, G. A., Davidson, M. J., & Nokes, R. I. (2007). Inclined negatively buoyant discharges. *Journal of Hydraulic Engineering Division of the American Society of Civil Engineers*, 133(5), 545–554.

- Koochesfahani, M. M., & Dimotakis, P. E. (1985). Laser-induced fluorescence measurements of mixed fluid concentration in a liquid plane shear layer. *AIAA Journal*, 23(11), 1700–1707.
- Kwon, S. J., & Seo, I. W. (2005). Experimental investigation of wastewater discharges from a Rosette-type diffuser using PIV. *KSCE Journal of Civil Engineering*, 9(5), 355–362.
- Lai, A. C. H., & Lee, J. H. W. (2012). Dynamic interaction of multiple buoyant jets. *Journal of Fluid Mechanics*, 708, 539–575.
- Lane-Serff, G. F., Linden, P., & Hillel, M. (1993). Forced, angled plumes. *J. Hazardous Materials*, 33(1), 75–99.
- Lattemann, S., & Höpner, T. (2008). Environmental impact and impact assessment of seawater desalination. *Desalination*, 220(1–3), 1–15.
- Law, A. W.-K., Lee, C. C., & Qi, Y. (2002). CFD modeling of a multi-port diffuser in an oblique current. In *MWWD2002*, Istanbul, Turkey, September 16–20, 2002.
- Lindberg, W. R. (1994). Experiments on negatively buoyant jets, with and without cross-flow. In *NATO Advanced Research Workshop on “Recent Advances in Jets and Plumes” NATO ASI Series E* (Vol. 255, pp. 131–145). Viana do Castelo, Portugal: Kluwer Academic Publishers.
- Marti, C. L., Antenucci, J. P., Luketina, D., Okely, P., & Imberger, J. (2011). Near-field dilution characteristics of a negatively buoyant hypersaline jet generated by a desalination plant. *Journal of Hydraulic Engineering Division of the American Society of Civil Engineers*, 137(1), 57–65.
- Miller, B. M., Glamore, W. C., Timms, W. A., & Pells, S. E. (2006). *Physical modeling of desalination brine outlet, Perth (Stage 2)*. The University of New South Wales, School of Civil and Environmental Engineering, Water Research Laboratory.
- Miller, B., & Tarrade, L. (2010). Design considerations of outlet discharges for large seawater desalination projects in Australia. In *6th International Conference on Marine Wastewater Discharges, MWWD 2010*, Langkawi, Malaysia, October 25–29, 2010.
- Muller, J., Seil, G., & Hubbert, G. (2011). Three modelling techniques used in Australia to model desalination plant brine dispersal in both the near-field and far-field. In *International Symposium on Marine Outfall Systems*, Mar del Plata, Argentina, May 15–19, 2011.
- Oliver, C. J., Davidson, M. J., & Nokes, R. I. (2008). k- ϵ predictions of the initial mixing of desalination discharges. *Environmental Fluid Mechanics*, 8, 617–625.
- Palomar, P., Lara, J. L., & Losada, I. J. (2012a). Near field brine discharge modeling part 2: Validation of commercial tools. *Desalination*, 290(0), 28–42.
- Palomar, P., Lara, J. L., Losada, I. J., Rodrigo, M., & Álvarez, A. (2012b). Near field brine discharge modelling part 1: Analysis of commercial tools. *Desalination*, 290, 14–27.
- Pincince, A. B., & List, E. J. (1973). Disposal of brine into an estuary. *Journal of WPCF*, 45(11), 2335–2344.
- Roberts, P. J. W., Ferrier, A., & Daviero, G. J. (1997). Mixing in inclined dense jets. *Journal of Hydraulic Engineering Division of the American Society of Civil Engineers*, 123(8), 693–699.
- Roberts, P. J. W., & Abessi, O. (2014). *Optimization of desalination diffusers using three-dimensional laser-induced fluorescence*. Final Report Prepared for United States Bureau of Reclamation. Georgia Tech, Atlanta, Georgia.
- Roberts, D. A., Johnston, E. L., & Knott, N. A. (2010). Impacts of desalination plant discharges on the marine environment: A critical review of published studies. *Water Research*, 44(18), 5117–5128.
- Roberts, P. J. W., & Snyder, W. H. (1993). Hydraulic model study for the Boston Outfall. II: Environmental performance. *Journal of Hydraulic Engineering Division of the American Society of Civil Engineers*, 119(9), 988–1002.
- Roberts, P. J. W., Snyder, W. H., & Baumgartner, D. J. (1989). Ocean outfalls. I: Submerged wastefield formation. *Journal of Hydraulic Engineering Division of the American Society of Civil Engineers*, 115(1), 1–25.
- Roberts, P., Jenkins, S., Paduan, J., Schlenk, D., & Weis, J. (2012). *Management of brine discharges to coastal waters: Recommendations of a science advisory panel*. Environmental Review Panel (ERP). Southern California Coastal Water Research Project (SCCWRP). Costa Mesa, CA. Technical Report 694. http://www.swrcb.ca.gov/water_issues/programs/ocean/desalination/docs/dpr.pdf.

- Seil, G., & Zhang, Q. (2010). CFD modeling of desalination plant brine discharge systems. *Water*, September 2010, 79–83.
- Smith, R., Purnama, A., & Al-Barwani, H. H. (2007). Sensitivity of hypersaline Arabian Gulf to seawater desalination plants. *Applied Mathematical Modelling*, 31(10), 2347–2354.
- Sofianos, S., Johns, W. E., & Murray, S. (2002). Heat and freshwater budgets in the Red Sea from direct observations at Bab el Mandeb. *Deep Sea Research Part II: Topical Studies in Oceanography*, 49(7–8), 1323–1340.
- Sotiropoulos, F. (2005). Introduction to statistical turbulence modeling for hydraulic engineering flows. In P. D. Bates, S. N. Lane, & R. I. Ferguson (Eds.), *Computational fluid dynamics*. New York: Wiley.
- Tang, H. S., Paik, J., Sotiropoulos, F., & Khangaonkar, T. (2008). Three-dimensional numerical modeling of initial mixing of thermal discharges at real-life configurations. *Journal of Hydraulic Engineering Division of the American Society of Civil Engineers*, 134(9), 1210–1224.
- Tarrade, L., & Miller, B. M. (2010). *Physical modeling of the victorian desalination plant outfall*. The University of New South Wales, School of Civil and Environmental Engineering, Water Research Laboratory.
- Tian, X., & Roberts, P. J. W. (2003). A 3D LIF system for turbulent buoyant jet flows. *Experiments in Fluids*, 35, 636–647.
- Tian, X., Roberts, P. J. W., & Daviero, G. J. (2004). Marine wastewater discharges from multiport diffusers I: Unstratified stationary water. *Journal of Hydraulic Engineering Division of the American Society of Civil Engineers*, 130(12), 1137–1146.
- Tian, X., & Roberts, P. J. W. (2011). Experiments on marine wastewater diffusers with multiport Rosettes. *Journal of Hydraulic Engineering Division of the American Society of Civil Engineers*, 137(10), 1148–1159.
- Zhang, X. Y., & Adams, E. E. (1999). Prediction of near field plume characteristics using a far field circulation model. *Journal of Hydraulic Engineering Division of the American Society of Civil Engineers*, 125(3), 233–241.